

# Spin dynamics of $\text{Sr}_{14}\text{Cu}_{24}\text{O}_{41}$ two-leg ladder studied by Raman spectroscopy

A. Gozar<sup>1,2</sup>, G. Blumberg<sup>1,†</sup>, B.S. Dennis<sup>1</sup>, B.S. Shastry<sup>1</sup>, N. Motoyama<sup>3</sup>, H. Eisaki<sup>4</sup>, and S. Uchida<sup>3</sup>

<sup>1</sup>*Bell Laboratories, Lucent Technologies, Murray Hill, NJ 07974*

<sup>2</sup>*University of Illinois at Urbana-Champaign, Urbana, IL 61801-3080*

<sup>3</sup>*The University of Tokyo, Bunkyo-ku, Tokyo 113, Japan*

<sup>4</sup>*Stanford University, Stanford, CA94305*

(April 2, 2001; Accepted for Physical Review Letters)

The two-magnon (2M) excitation at  $3000 \text{ cm}^{-1}$  in  $\text{Sr}_{14}\text{Cu}_{24}\text{O}_{41}$  two-leg ladder is studied by Raman scattering. A slight anisotropy of the superexchange coupling  $J_{\perp}/J_{\parallel} \approx 0.8$  with  $J_{\parallel} = 110 \pm 20 \text{ meV}$  is proposed from the analysis of the magnetic scattering. The resonant coupling across the charge transfer gap increases the 2M intensity by orders of magnitude. The anisotropy of Raman scattering is dependent upon the excitation energy. The 2M relaxation is found to be correlated with the temperature dependent electronic Raman continuum at low frequencies.

PACS numbers: 74.72.Jt, 78.30.-j, 75.40.Gb, 75.10.Jm

*Introduction.*— Spin dynamics of low-dimensional copper oxide materials with spin  $S=1/2$  copper ions is attracting much attention because of the critical nature of the ground state and its possible relevance to the phase diagram of high temperature superconducting cuprates [1,2]. Quantum fluctuations in the  $S=1/2$  Heisenberg one-dimensional (1D) antiferromagnetic (AF) linear chain  $H_{\parallel} = J_{\parallel} \sum_{\text{leg}} (\mathbf{S}_i \cdot \mathbf{S}_j - \frac{1}{4})$  are so strong that the ground state is disordered and gapless [3]. The excitations from the ground state are  $S=1/2$  topological kinks (solitons) called *spinons*. Two chain coupling in two-leg ladder structures is described by the spin Hamiltonian  $H = H_{\perp} + H_{\parallel}$ , where  $H_{\perp} = J_{\perp} \sum_{\text{rung}} \mathbf{S}_i \cdot \mathbf{S}_j$  is the interchain coupling. If the AF coupling across the rung  $J_{\perp}$  is much larger than  $J_{\parallel}$ , the ground state consists of spin singlets, one on each rung, with a gap  $\Delta \approx J_{\perp}$  to the lowest triplet spin excitation. A finite  $J_{\parallel}$  will drive the system into a resonating valence bond (RVB) state [4–8] with a finite spin gap for any value of the ratio  $r = J_{\perp}/J_{\parallel}$ . The RVB state is a coherent superposition of valence bonds. For even leg ladders the RVB states are short ranged and can be visualized as predominantly interchain singlets with resonances to include intrachain singlets. The elementary excitations out of the RVB ground state are  $S = 1/2$  quasiparticles that carry no charge. They are viewed as topological defects that can be created or destroyed only in pairs by breaking a singlet bond. Gradual introduction of interladder coupling drives the system from the quantum RVB state to a magnetically ordered 2D Néel state with classical spin-wave excitations [9].

$\text{Sr}_{14}\text{Cu}_{24}\text{O}_{41}$  is an experimental realization of a two leg ladder structure. The planes of  $\text{Cu}_2\text{O}_3$  weakly coupled ladders are stacked along the  $b$  crystallographic axis alternating with 1D  $\text{CuO}_2$  edge-sharing chain sheets [10,11]. The legs and rungs of the ladders are along the  $c$  and  $a$  crystallographic axes. This compound is intrinsically doped and the holes are believed to reside mainly in the chain substructure [12]. The spin dynamics in the ladders

is governed by the ratio  $r$  of the magnetic exchange across and along the legs. INS and NMR measurements suggest superexchange energies  $J_{\perp} \approx 72 - 80 \text{ meV}$  and  $r \approx 0.5$  [13,14] while Raman measurements derived values close to the isotropic limit for  $J_{\perp}$  and  $J_{\parallel}$  [15].

In this Letter we study resonant magnetic Raman scattering from  $\text{Sr}_{14}\text{Cu}_{24}\text{O}_{41}$  which provides information about the spin dynamics from the two-magnon (2M) peak position and shape [16]. The 2M feature, which displays distinct characteristics from the corresponding excitation in 2D cuprate materials, is analyzed as a function of temperature, polarization and incoming photon energy. From the energy of the 2M resonance and the value of the spin gap we suggest  $r = 0.8 \pm 0.1$  and  $J_{\parallel} = 110 \pm 20 \text{ meV}$ . The temperature dependence of the magnetic scattering is found to be correlated with the suppression of the low frequency Raman continuum and the redistribution of states seen in optical absorption, reflecting that the low-energy spin-dynamics is driven by temperature dependent high energy interactions.

*Experimental.*— Single crystals of  $\text{Sr}_{14}\text{Cu}_{24}\text{O}_{41}$  were grown as described in [12,17]. Raman measurements were performed from the *ac* surface of the crystal mounted in a continuous helium flow optical cryostat. Spectra were taken in a backscattering geometry using linearly polarized excitations of a  $\text{Kr}^+$  laser from IR to violet. An incident laser power less than 3 mW was focused to a  $50 \mu\text{m}$  spot onto the sample surface. The spectra were analyzed by a custom triple grating spectrometer and the data were corrected for the spectral response of the spectrometer and the detector as well as for the optical properties of the material at different wavelengths as described in [18,19].

*Magnetic scattering.*— In Fig. 1 we present low-temperature magnetic Raman scattering spectra from  $\text{Sr}_{14}\text{Cu}_{24}\text{O}_{41}$  for (cc) and (aa) polarizations. The data is taken in the pre-resonant regime (1.84 eV excitation). The peak at  $3000 \text{ cm}^{-1}$  (375 meV) is assigned to a photon induced spin exchange or 2M excitation. The 2M reso-

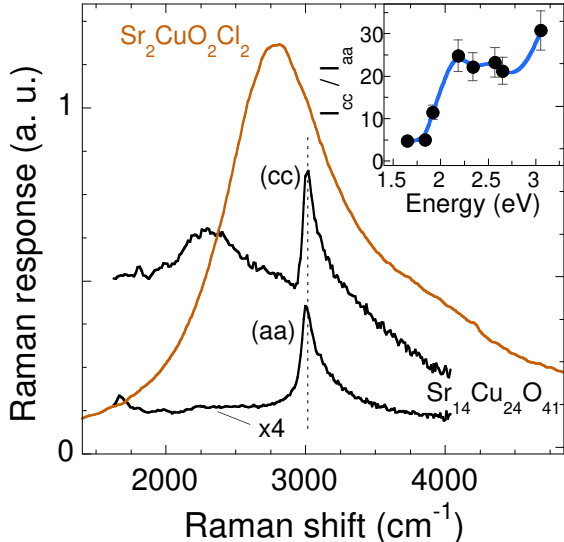


FIG. 1. Low temperature Raman response function in (cc) and (aa) polarization for  $\text{Sr}_{14}\text{Cu}_{24}\text{O}_{41}$  with  $\omega_{in} = 1.84$  eV excitation. The broad feature is 2M excitation for 2D AF insulator  $\text{Sr}_2\text{CuO}_2\text{Cl}_2$  with  $\omega_{in} = 2.73$  eV. Inset: the relative intensity of the 2M excitation in (cc) *vs.* (aa) polarization as a function of the incoming photon energy (from Fig. 4). The solid line is a guide to the eye.

nance is a sharp asymmetric feature with a tail at higher frequencies. In (aa) polarization the peak is about four times weaker than in (cc) polarization and is found at the same energy. A semi-classical counting of broken magnetic bonds within a local Néel environment as shown in Fig. 2a-b was proposed to describe the spin exchange process and determine  $J_{||}$  and  $J_{\perp}$  [15]. For anisotropic coupling along and across the legs a simple Ising counting leads to different peak energies in the (aa) and (cc) polarizations which we did not observe. The isotropic case estimates  $J \approx 200$  meV which is almost 50% higher than in related cuprate materials.

An RVB description of the ladder ground state has been suggested [7]. Fig. 2c-d is a cartoon of the local magnetic excitation within this approach. Starting from an "instantaneous" configuration of the ground state, (Fig. 2c), during the Raman process two neighboring singlets get excited into a higher singlet state of two bound triplets (Fig. 2d).

An effective spin interaction leading to the 2M light scattering was first developed by Loudon and Fleury [20]. For Mott-Hubbard systems the photon induced spin exchange formalism was developed in pre-resonant [21] and resonant [22] regimes. In our notation  $\mathbf{e}_{in}$  and  $\mathbf{e}_{out}$  are the polarization vectors of the incoming and scattered light, and  $\theta$  is the the angle between  $\mathbf{e}_{in}$  and the  $a$ -axis. For  $\mathbf{e}_{in} \parallel \mathbf{e}_{out}$ , considering nearest neighbor exchange and taking into account the anisotropy of the coupling constants denoted by  $A$  and  $B$  [23], the light scattering interaction is:

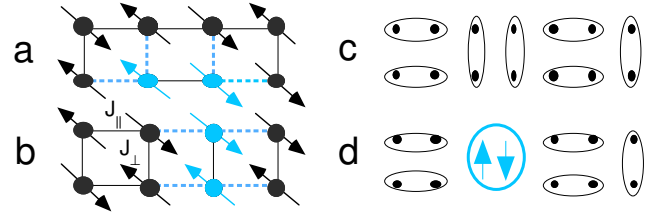


FIG. 2. Cartoon showing the magnetic excitation assuming a local Néel (a, b) or a RVB (c, d) description of the ladders. The spin exchange shown in lighter shades is along (a) and across (b) ladder legs. (c) - a particular valence-bond configuration in the ladder ground state; (d) - locally excited singlet state of two bound triplet excitations.

$$H_{LS} = A \sin^2(\theta) \sum_{leg} \mathbf{S}_i \cdot \mathbf{S}_j + B \cos^2(\theta) \sum_{rung} \mathbf{S}_i \cdot \mathbf{S}_j \quad (1)$$

Using the relationship between  $H_{LS}$  and the nearest-neighbor Heisenberg ladder Hamiltonian, the following angular dependence of the 2M intensity for  $\mathbf{e}_{in} \parallel \mathbf{e}_{out}$  can be found:

$$I_{||}(\omega, \theta) = I_{||}(\omega, 0) [\cos^2(\theta) - \frac{A}{B} r \sin^2(\theta)]^2 \quad (2)$$

The ratio of the 2M peak intensity in parallel polarization along and across the ladder allows the extraction of the exchange anisotropy if the  $A$  to  $B$  ratio is known. In resonance the  $A/B$  value is excitation energy dependent and it approaches a constant value in the pre-resonant regime [21]. This can be seen in the inset of Fig. 1 where we show the ratio of the 2M intensity for (cc) and (aa) polarizations as a function of  $\omega_{in}$ .

The constraints imposed by the 2M energy at  $3000 \text{ cm}^{-1}$  measured by Raman and the spin gap value  $\Delta = 32$  meV measured by INS [13] allow us to estimate  $J_{||}$  and  $J_{\perp}$ . Numerical calculations suggest that most of the 2M Raman spectral density at  $k = 0$  arises from the combination of triplets with wavevectors close to the Brillouin Zone (BZ) center [24]. In that region the elementary magnons are weakly dispersive and the resonance situated around twice that energy reflects the singularities in the single particle density of states. We estimate  $r = 0.8 \pm 0.1$  and  $J_{||} = 110 \pm 20$  meV, the error bars allowing for effects induced by the presence of ring exchange [25] and finite state interaction. A slightly anisotropic  $r$  may be due to the difference in the lattice constants along the  $a$  and  $c$  axes as well as from the anisotropy of the Cu-O-Cu bonds [26]. From Eq. (2) we obtain the ratio of the coupling constants  $A/B \approx 2.5$  in the pre-resonant regime, which would be compatible with an anisotropic local Cu  $d$  - O  $p$  excitation and slightly different hopping parameters [27] along and across the ladder.

*Two-magnon relaxation.*— To emphasize the 2M sharpness we compare it to the corresponding excitation in  $\text{Sr}_2\text{CuO}_2\text{Cl}_2$  which has the sharpest 2M feature among

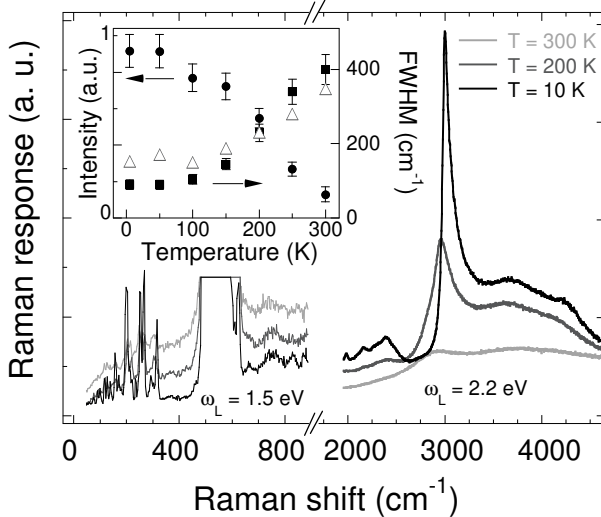


FIG. 3. Temperature dependent Raman spectra in (cc) polarization for  $\text{Sr}_{14}\text{Cu}_{24}\text{O}_{41}$ . Different energy scales were used for the two excitation regimes. Left:  $\omega_{in} = 1.5$  eV (the phonons around  $550 \text{ cm}^{-1}$  are truncated). Right:  $\omega_{in} = 2.2$  eV where the 2M peak at  $3000 \text{ cm}^{-1}$  is shown for three temperatures. Inset: the integrated intensity of the 2M peak (circles, left scale) and the FWHM (filled squares, right scale). The triangles represent the continuum intensity around  $700 \text{ cm}^{-1}$ .

2D AF copper oxides [28]. In the latter case the full width at half maximum (FWHM) is about  $800 \text{ cm}^{-1}$  [28,29] while for  $\text{Sr}_{14}\text{Cu}_{24}\text{O}_{41}$  the FWHM is about  $90 \text{ cm}^{-1}$ .

For the 2D cuprates the experimental Raman spectrum shows significant deviations from calculations within the 2D Heisenberg model. Calculations within spin-wave theory [16,30] reproduce the 2M profile peaked below  $3J$  which is in good agreement with the experiments. However, the large width of the experimental spectra has not been reproduced within the standard spin-wave model. The narrow calculated width of the 2M peak was found to be stable with respect to inclusion of the higher order spin interactions [30]. Intrinsic inhomogeneities were suggested to be responsible for the anomalous 2M width in 2D cuprates [31]. A recent quantum Monte Carlo calculation of Sandvik *et al.* [32] reproduced a 2M profile broader than that obtained within the spin-wave theory but still narrower than typical experimental spectra. Authors of the latter work considered the broadening as support to the earlier claim by Singh *et al.* [33] that the broadening is due to the strong quantum fluctuations of the Heisenberg model with  $S = 1/2$ . It is interesting to note, however, that for the  $S = 1/2$  quasi-1D ladder structure the 2M profile is narrow. This experimental result questions the broadening argument for 2D cuprates due to quantum fluctuations. The major difference in the 2M width between 2D cuprates and the spin ladders is due to the suppression of the magnetic relaxation channels in the gapped quasi-1D weakly coupled ladder system.

*Two-magnon temperature dependence.*— The 2M peak

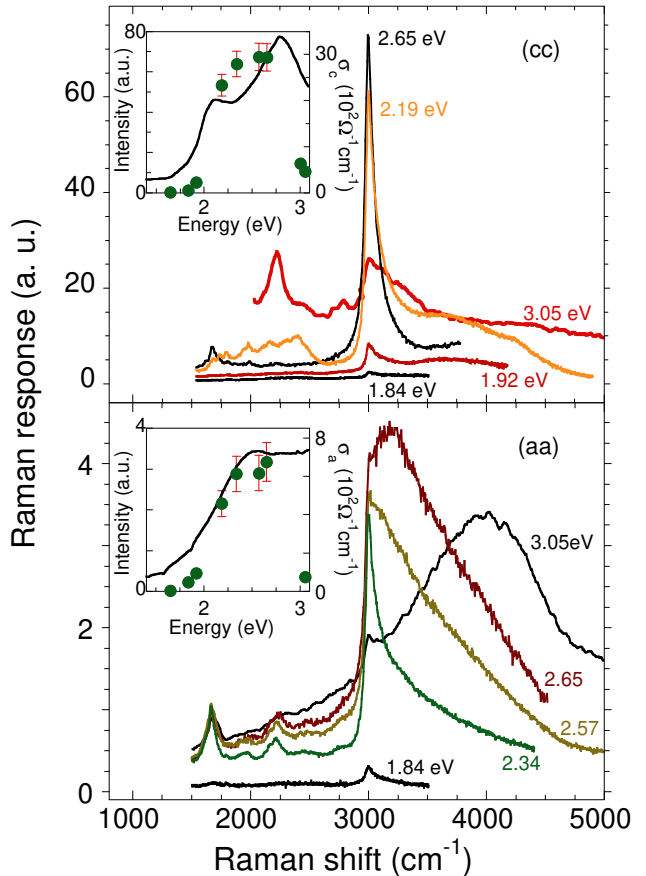


FIG. 4. Upper panel: Raman response for  $\text{Sr}_{14}\text{Cu}_{24}\text{O}_{41}$  in (cc) polarization at  $T = 10$  K, for different excitation energies. Inset: the resonance profile of the 2M peak (filled circles, left scale), and the c-axis optical conductivity (solid line, right scale). Lower panel: The same data for the (aa) polarization; in the inset the solid line represents the a-axis optical conductivity.

is weak and heavily damped at room temperature (Fig. 3). Upon cooling we notice two main features: first, the spectral weight increases by almost an order of magnitude and second, the 2M peak sharpens from about  $400$  to  $90 \text{ cm}^{-1}$  FWHM at  $T = 10\text{K}$ . Because  $J/k_B T$  remains large even at room temperature, the observed effects are surprising. In 2D cuprates, for example, the 2M peak remains well defined above  $600$  K [29].

The electronic continuum shown in Fig. 3 for energies below  $1000 \text{ cm}^{-1}$  gets suppressed with cooling. The presence of low lying states at high temperatures is confirmed by NMR [34] and also in measurements of c-axis conductivity [19]. In the latter case a gap-like feature below  $1 \text{ eV}$  develops with cooling and the low energy spectral weight gets transferred to energies between  $2$  and  $3 \text{ eV}$ .

As seen in the inset of Fig. 3 the increase of the electronic Raman background with heating is correlated with the damping of the 2M peak. The introduced low energy states reduce the lifetime of the magnetic excitation by providing additional relaxational channels. We may spec-

ulate that the states are provided *via* the small amount of self-doped carriers in the ladder subsystem [35]. The strengthening of the 2M seen with the 2.2 eV excitation energy might be related to the enhancement of about 30% of the optical conductivity around this energy.

*Two-magnon excitation profile.*— The superexchange mechanism involves hopping of electrons to the nearest neighbors sites *via* the intermediate oxygen  $2p$  orbitals. Therefore we expect a change in the 2M band intensity and shape as the incoming photon energy approaches the charge-transfer (CT) gap. Fig. 4 shows the Raman response for  $\text{Sr}_{14}\text{Cu}_{24}\text{O}_{41}$  for different excitation energies. The 2M resonant Raman excitation profile is plotted in the insets along with the optical conductivity data. For both the (cc) and (aa) polarizations the resonant enhancement has a maximum around 2.7 eV, about 0.7 eV higher than the CT edge seen in the optical conductivity. The intensity is small for  $\omega_{in} < 2$  eV and increases monotonically as the photon energy becomes comparable to the CT gap followed by a drop for excitations about 3 eV. The 2M profile displays an orders of magnitude increase in intensity as the incident photon energy is varied in the visible spectrum. As in the cuprate materials [22] a resonant Raman coupling has to be considered in order to quantitatively understand the experimental observations. Noticeably the 2M acquires an excitation dependent sideband as can be seen in Fig. 4. In the (aa) polarization it appears for photon energies higher than 2.4 eV corresponding to the edge seen in the  $a$ -axis conductivity [36].

*Summary.*— We studied the 2M excitation at  $3000 \text{ cm}^{-1}$  in two-leg ladders by Raman scattering. Resonant coupling across the CT gap at about 2 eV increases the magnetic scattering intensity by orders of magnitude. At low temperatures the 2M is a well defined resonance with a FWHM of  $\approx 90 \text{ cm}^{-1}$ , much sharper than the 2M band in 2D cuprates. From the temperature dependence of the 2M width we find that the magnetic relaxation is caused by excitations seen in the low-frequency electronic Raman continuum and the optical conductivity as the temperature is raised. The presence of holes in the ladder subsystem is at the origin of this continuum. A slight anisotropy in the ladder exchange due to geometrical factors  $r = J_{\perp}/J_{\parallel}$  of about 0.8 is derived from the analysis of our data. We show that the light coupling to the magnetic excitations is anisotropic and excitation dependent.

We would like to acknowledge discussions with M.V. Klein, A.M. Sengupta, R.R. Singh and S. Trebst.

- [3] L.D. Faddeev and L.A. Takhtajan, Phys. Lett. A **85**, 375 (1981).
- [4] E. Dagotto and T.M. Rice, Science **271**, 618 (1996).
- [5] T. Barnes, E. Dagotto, J. Riera, and E.S. Swanson, Phys. Rev. B **47**, 3196 (1993).
- [6] J. Oitmaa, R. R. P. Singh, and Z. Weihong, Phys. Rev. B **54**, 1009 (1996) and references therein.
- [7] S. R. White, R. M. Noack and D. J. Scalapino Phys. Rev. Lett. **73**, 886 (1994).
- [8] S. Kivelson *et al.*, Phys. Rev. B **35**, 8865 (1987).
- [9] S. Sachdev, Science **288**, 475 (2000).
- [10] E. M. McCarron *et al.*, Mater. Res. Bull. **23**, 1355 (1988).
- [11] T. Siegrist *et al.*, Mater. Res. Bull. **23**, 1429 (1988).
- [12] T. Osafune *et al.*, Phys. Rev. Lett. **78**, 1980 (1997).
- [13] R. S. Eccleston *et al.*, Phys. Rev. Lett. **81**, 1702 (1998).
- [14] T. Imai *et al.*, Phys. Rev. Lett. **81**, 220 (1998).
- [15] S. Sugai and M. Suzuki, Phys. Stat. Sol. (b) **215**, 653 (1999).
- [16] R. J. Elliott and M. F. Thorpe, J. Phys. C **2**, 1630 (1969); J. B. Parkinson, J. Phys. C **2**, 2012 (1969).
- [17] N. Motoyama *et al.*, Phys. Rev. B **55**, R3386 (1997).
- [18] G. Blumberg *et al.*, Phys. Rev. B **49**, R13295 (1994).
- [19] N. Motoyama and H. Eisaki, private communications.
- [20] P. A. Fleury and R. Loudon, Phys. Rev. **166**, 514 (1968).
- [21] B. S. Shastry, and B. I. Shraiman, Phys. Rev. Lett. **65**, 1068 (1990).
- [22] A. V. Chubukov and D. M. Frenkel, Phys. Rev. Lett. **74**, 3057 (1995).
- [23] S. Sugai, in *Magneto-Optics*, eds. S. Sugano and N. Kojima (Springer, Berlin, 2000), p. 75.
- [24] C. Knetter *et al.*, cond-mat/0106077.
- [25] M. Matsuda *et al.*, Phys. Rev. B **62**, 8903 (2000).
- [26] T. Ohta *et al.*, J. Phys. Soc. Jpn. **66**, 3107 (1997).
- [27] T. F. A. Muller *et al.*, Phys. Rev. B **57**, R12655 (1998).
- [28] G. Blumberg *et al.*, Phys. Rev. B **53**, R11930 (1996).
- [29] P. Knoll *et al.*, Phys. Rev. B **42**, 4842 (1990).
- [30] C.M. Canali and S.M. Girvin, Phys. Rev. B **45**, 7127 (1992).
- [31] F. Nori *et al.*, Phys. Rev. Lett. **75**, 553 (1995).
- [32] A.W. Sandvik *et al.*, Phys. Rev. B **57**, 8478 (1998).
- [33] R.R.P. Singh *et al.*, Phys. Rev. Lett. **62**, 2736 (1989).
- [34] M. Takigawa *et al.*, Phys. Rev. B **57**, 1124 (1998).
- [35] T. Takahashi *et al.*, Phys. Rev. B **56**, 7870 (1997).
- [36] Additional interactions, for example multimagnon or multiphonon scattering, in the intermediate excited fermionic state, render this process dependent on the higher bands dispersions.

<sup>†</sup> Corresponding author, e-mail: girsh@bell-labs.com

- [1] P.W. Anderson, Science **235**, 1196 (1987).
- [2] T. Senthil and M.P.A. Fisher, Phys. Rev. Lett. **86**, 292 (2001).